IEEE Photonics Journal
An IEEE Photonics Society Publication

Solar Scintillation Effect for Optical Waves Propagating Through Gamma–Gamma Coronal Turbulence Channels

Volume 11, Number 4, August 2019

Guanjun Xu, ***Member, IEEE***
Min Zeng

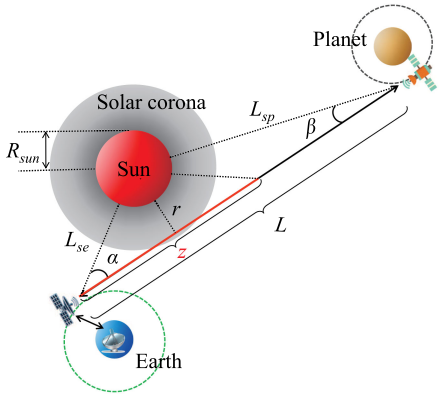

DOI: 10.1109/JPHOT.2019.2924039

Solar Scintillation Effect for Optical Waves Propagating Through Gamma–Gamma Coronal Turbulence Channels

Guanjun Xu [1,2,3] ***Member, IEEE***, **and Min Zeng**[4]

[1]School of Information Science and Technology, East China Normal University, Shanghai 200241, China
[2]Engineering Center of SHMEC for Space Information and GNSS, East China Normal University, Shanghai 200241, China
[3]Shanghai Key Laboratory of Multidimensional Information Processing, East China Normal University, Shanghai 200241, China
[4]College of Information Engineering, Southwest University of Science and Technology, Mianyang 621010, China

DOI:10.1109/JPHOT.2019.2924039

Manuscript received May 6, 2019; revised June 9, 2019; accepted June 17, 2019. Date of publication June 20, 2019; date of current version July 15, 2019. This work was supported in part by the National Natural Science Foundation of China under Grants 61801181 and 61831008 and in part by the Open Research Fund of Shanghai Key Laboratory of Multidimensional Information Processing, East China Normal University. Corresponding author: Guanjun Xu (e-mail: gjxu@ee.ecnu.edu.cn).

Abstract: Optical communication is a promising strategy for deep space exploration but it is susceptible to coronal solar wind turbulence impairments during superior solar conjunction. The variance of amplitude fluctuations caused by coronal turbulence on optical waves propagation is proposed in this paper. Both the generalized non-Kolmogorov coronal turbulence spectrum and the aperture averaging effect are taken into account. The analytic expression of the bit error rate (BER) for free-space optical (FSO) link is then derived based on Gamma–Gamma distribution model under the weak-to-moderate coronal turbulence channels. Numerical evaluations results demonstrate that coronal turbulence with small non-Kolmogorov spectral index, large outer scale, and inner scale has more potential to deduce amplitude fluctuations. With the increment of antenna radius, the amplitude fluctuations decrease obviously. In addition, the variation tendencies of these parameters can further result in small BER. Therefore, the link performance will be improved by decreasing the optical wavelength and enlarging the antenna radius. Our proposed amplitude fluctuations model with aperture averaging effect has potential application for the future deep space FSO communication.

Index Terms: Coronal turbulence, superior solar conjunction, amplitude fluctuations, scintillation index, spectral index, bit error rate (BER).

1. Introduction

Compared with the microwave communication, free-space optical (FSO) communication has found wide applications in many communication scenarios, thanks to its extensive advantages, such as higher data rate, faster link installation, larger bandwidth, and lower power consumption, and so on. The successful application of optical communication in satellite links and inter-satellite links makes it possible to use this technology in deep space communication. With the rapid development of deep space exploration, a new era of study on FSO communication in deep space is becoming

increasingly urgent and is of widespread concern [1], [2]. In view of the considerable transmission delay and signal attenuation induced by the ultra-long distance in deep space FSO communication, considerable efforts have been devoted to handle these issues in the exploration missions and they have obtained fruitful results. In addition to these severe impacts on FSO communication link performance, the link will also suffer from solar scintillation induced by coronal solar wind turbulence during superior solar conjunction when the Sun lies between the Earth and the spacecraft [3]. The solar scintillation, which is referred to wave scattering, is directly related to amplitude fluctuations, phase fluctuations, and angle-of-arrival fluctuations, due to the random changes in refractive index. Under this circumstance, the optical beam quality will be severely reduced and this resulting in high bit error rate (BER). Thereafter, the link performance degraded seriously and the communication link can even be interrupted during this period. Consequently, a better understanding and evaluation of the solar scintillation effect on the FSO communication link is crucial before we can design future deep space missions.

In recent years, many researchers have devoted themselves to evaluating the solar scintillation effect on the deep space communication link. A fitted solar scintillation index model was first proposed by Feria *et al.* with the observation data of solar scintillation effect on X and Ka band signal [4]. This model has since been applied in the prediction of amplitude fluctuations and provided potential application for the link performance calculation under Rician channel model [5], [6]. Unfortunately, this model neglects the inherent relationship between the scintillation intensity and the turbulent solar wind plasma with a wide range scale. Therefore, its accuracy urgently needs be improved with a solid theory foundation. Morabito *et al.* elaborated the solar scintillation effect for Cassini 2000 during its superior solar conjunction and proposed the scintillation index model based on the conventional scattering theory with the Kolmogorov spectrum model [7]. Considering the weak scintillation case, both the amplitude fluctuations and the scintillation index model were derived based on the Rytov approximation theory in [8]. Their results demonstrated that these models achieve high accuracy and the scintillation has a closely relationship with the outer scale. Even though the solar scintillation has been discussed extensively, it was only carried out with the Kolmogorov spectrum model. However, the actual coronal spectrum is non-Kolmogorov and the spectral index ranges from 3 to 4 according to the astronomical observation [9]. Meanwhile, Efimov *et al.* developed a closed-form scintillation index model with a non-Kolmogorov coronal turbulent spectrum model [10]. The results of their study prove that the scintillation effect has an intricate relationship with the spectral index. In addition, the scintillation index increase dramatically at a heliocentric distance of about four solar radii. In our earlier research, both the amplitude fluctuations and phase fluctuations models have been proposed for radio waves propagation in coronal turbulence with the heliocentric distance is confined to four solar radii [11], [12]. These proposed solar scintillation models can not only be used to predict the scintillation intensity but also have potential advantages in investigating the coronal parameters [13], [14].

Although many efforts have been made in exploiting the amplitude fluctuations or solar scintillation index model, they are constrained to the radio frequency communication during superior solar conjunction. The effect of solar scintillation on optical waves propagation has seldom been analyzed to the best of our knowledge. In addition, the link performance under solar scintillation effect for optical communication during superior solar conjunction has not been fully investigated.

According to the variation of scintillation intensity, the scintillation is normally divided into a wide range regimes, such as weak scintillation, weak-to-moderate scintillation, strong scintillation, and saturation scintillation. With the assumption of weak scintillation, the BER performance of optical waves propagation under lognormal (LN) distribution coronal turbulence has been investigated based on our derived scintillation index model [11]. After that, a coperehensive investigation about the solar scintillation effect on deep space FSO communication is given by us in [15], and we further used the pulse-postion modulation (PPM) to improve the link performance under LN channel [16]. Although the LN distribution has been widely used for the BER analysis for optical waves propagation in atmospheric turbulence and ocean turbulence, it is only applicable for the weak turbulence condition. The optical signal will inevitably suffer multiple scattering effects when the strength of turbulence increases. Therefore, the BER performance with LN distribution exhibits large

deviation which has been reported in [17]. Compared with the measurement data, the BER with LN distribution will be also underestimated in the tails [18]. Therefore, this distribution model may not be appropriable for moderate and even strong scintillation. Given the limitations of LN distribution model, the Gamma-Gamma (GG) distribution model has been proposed to characterize the turbulence channel with the advantage being applicable for a wide range of turbulence intensities, such as weak-to-moderate scintillation [19]. Uysal *et al.* investigated the BER performance for coded FSO link over GG atmospheric turbulence channels [18]. Considering the GG atmospheric turbulence channels, Wang *et al.* further employed the circular polarization shift keying schemes to improve the FSO link performance [20]. In brief, the link performance of optical waves in atmospheric turbulence has been investigated maturely under the weak scintillation and weak-to-moderate scintillation with the LN and GG distribution model, respectively. However, link performance for optical waves propagation in coronal turbulence under weak-to-moderate scintillation with the GG model is an urgent challenge that requires further investigation due to the development of state-of-the-art deep space optical communication.

To tackle these issues, we first introduce a deep space optical communication scheme during superior solar conjunction. The background model of the solar corona is presented carefully, such as the solar corona non-Kolmogorov spectrum model. After that, this paper proposes a closed-form amplitude fluctuations model and the BER prediction model for optical waves propagation in coronal turbulence. Our main contributions are summarized below.

- First, we derive a tractable expression for the amplitude fluctuations. To obtain more design insights, a closed-form expression for the variance of amplitude fluctuations is proposed by adopting some approximations and taking account the aperture averaging effect. These expressions reveal that the variation of turbulent outer scale, inner scale, spectral index, and antenna radius have an obvious impact on the amplitude fluctuations.
- Second, considering the link performance of optical waves propagation through coronal turbulence, which is a serious problem with the development of deep space exploration, we investigated the link BER with the assumption of weak-to-moderate scintillation under GG channel distribution model. The closed-form BER formula is further derived to facilitate the calculation.
- Finally, by numerical simulations, we depict that the proposed amplitude fluctuations model and BER model can well reveal the solar scintillation effect on the link performance. In addition, we show that our proposed BER model with GG channel model is preferable when the optical link suffers weak-to-moderate scintillation.

The outline of this paper is as follows. Section 2 briefly introduces the communication model and the non-Kolmogorov coronal turbulence model. Based on these models, the theoretical model for the amplitude fluctuations variance with aperture averaging effect is presented in Section 3. Section 4 further derives the BER formula for optical waves propagation under weak-to-moderate scintillation. The theoretical results are then investigated and discussed in Section 5. Finally, Section 6 provides conclusions while the proof is relegated to the Appendix.

2. Theoretical Model

2.1 Geometric Model of Superior Solar Conjunction

As described in Section 1, the optical communication will be used in the coming deep space exploration. Fig. 1 depicts one of the deep space communication schemes for a relay transmission between the Earth and target planet. During a long exploration time, the superior solar conjunction occurs periodically when the Earth, the Sun, and the planet become aligned. A geometric diagram for the superior solar conjunctions is given in Fig. 1. In this figure, a relay satellite is used between the ground station and the spacecraft. According to the potential architecture for future deep space communication, the radio signal first commutes between the ground station and the relay satellite via microwave, and then transmits between the relay satellite and the exploration spacecraft by optical wave. During superior solar conjunction, the deep space communication link will pass through

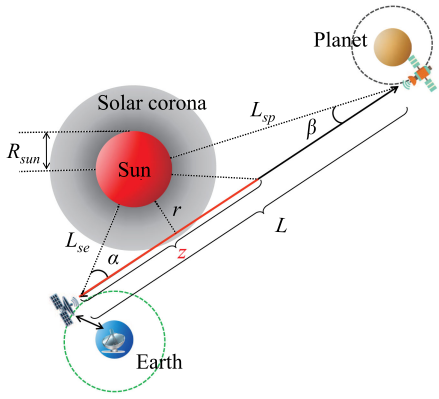

Fig. 1. Geometric diagram and communication architecture for deep space exploration during superior conjunction.

the solar corona and will encounter the coronal irregularities. Note that the coronal turbulence is constituted by the high density solar wind plasma, which erupts from the Sun and is transported to interplanetary space [3]. Due to the refractive index fluctuations of solar wind turbulence medium, the signal will be scattered, which is referred to as solar scintillation and, hence, the link performance deteriorates.

In this paper, we mainly consider about the effect of coronal solar wind turbulence on the optical waves propagation. The distance between the Sun and the communication link is called as heliocentric distance, r, which is introduced by astronomy. It should be emphasized the link distance, L, of the optical waves propagate between the relay satellite and the exploration spacecraft is assumed to be equal to the distance between the Earth and the planet, because it is so large compared with the distance between the satellite and the Earth during superior solar conjunction. According to the triangular relationship shown in Fig. 1, the link distance and the heliocentric distance can be obtained as

$$\begin{cases} L = L_{se}\cos\alpha + L_{sp}\cos\beta \\ r = z^2 + L_{se}^2 - 2zL_{se}\cos\alpha \end{cases}. \tag{1}$$

Here, α and β denote the Sun-Earth-Planet (SEP) angle and the Sun-Planet-Earth (SPE) angle, respectively. L_{sp} represents the distance between the Sun and the planet. In addition, z denotes the optical waves propagation distance. Note that, R_{sun} is used to represent the solar radius in this paper. In accordance with (1) and Fig. 1, the heliocentric distance decreases along with the increase of SEP angle and SPE angle. Therefore, the link will intuitively encounter more coronal turbulence and the link performance of optical waves prorogation through this turbulence degrades more seriously.

2.2 Generalized Refractive Index Fluctuation Spectrum for the Non-Kolmogorov Coronal Turbulence

Given that the solar wind erupts from the Sun stochastically and its density fluctuate both in spatial and temporal, it is quite difficult to directly characterize its inherent property. However, the solar wind spatial spectrum provides the potential to describe the solar wind turbulence irregularities. Several turbulence spectrum models have been proposed with the form $\Phi_N(\kappa) \propto \kappa^{-p}$, where κ is the spatial frequency vector and p denotes the spectral index. According to Taylor's frozen theory, the solar wind turbulence is a frozen random medium moving at the constant solar wind velocity. This assumption is reasonable and has been extensively used in radio astronomy research [21]. Relying on long-time observations and investigations, the coronal spectrum has been proved to be the non-Kolmogorov spectrum [21]. This phenomenon is more obvious in the near solar surface

regions with $r < 50R_{sun}$. Therefore, the spectral index is restricted with $3 < p < 4$ in this paper. According to [21], both the generalized exponential spectrum and the generalized von Karman turbulence spectrum are adopted to characterize the coronal turbulence spectrum model and can be expressed as

$$\Phi_N(\kappa, z) = C_N^2(r) \exp\left(-\kappa^2/\kappa_i^2\right)\left(\kappa_o^2 + \kappa^2\right)^{-p/2}, \tag{2}$$

Note that the coronal spectrum is directly related to the size of the turbulence eddies. $\kappa_o = 2\pi/L_o$, $\kappa_i = 2\pi/l_i$, L_o and l_i denote the outer scale and inner scale of the turbulence size, respectively. C_N^2 is the critical structure parameter used to characterize the turbulence strength of solar wind irregularities. According to [21], this has a close relationship with the solar wind density fluctuations, δN_e, and takes the following form

$$C_N^2(r) = \left\langle \delta N_e^2(r) \right\rangle \kappa_o^{p-3} \frac{(p-3)\,\Gamma\left(\frac{p}{2}\right)}{(2\pi)^{3/2}\Gamma\left(\frac{p-1}{2}\right)}. \tag{3}$$

where $\Gamma(\cdot)$ is the gamma function, $\langle\cdot\rangle$ denotes the ensemble average of realization.

It should be emphasized the actual solar wind fluctuations intensity is so complicated because the intricate corona environment has not yet been fully investigated. However, astronomical observations and studies prove that both the solar wind density and its fluctuation magnitude increase along with the decrease of the heliocentric distance [22]. Therefore, the solar wind fluctuations are generally simplified and assumed proportional to the solar wind plasma density, N_e, as

$$\left\langle \delta N_e(r) \right\rangle = \eta \left\langle N_e(r) \right\rangle, \tag{4}$$

where η is introduced to characterize the relative solar wind density fluctuation coefficient. Note that η increases quickly when the heliocentric distance decreases from $4R_{sun}$. In addition, $\delta N_e(r)$ can be also treated as a function of z according to (1).

To analyze the effect of solar wind density on the amplitude fluctuations, it is necessary to know the coronal solar wind density distribution, as well as the model describing solar wind density fluctuations. In this paper, we restrict the heliocentric distance in the range of $2R_{sun}$ to $4R_{sun}$. Therefore, we use the following solar wind density model, which has a high accuracy when $2R_{sun} < r < 20R_{sun}$ [23].

$$N_e(r) = 2.3 \times 10^8 \left(\frac{R_{sun}}{r}\right)^6 + 8.6 \times 10^6 \left(\frac{R_{sun}}{r}\right)^3 + 3.2 \times 10^5 \left(\frac{R_{sun}}{r}\right)^2, \tag{5}$$

By substituting (3) and (4) into (2), the coronal turbulence spectrum model can be finally recast as

$$\Phi_N(\kappa, z) = \eta^2 \left\langle N_e^2(r) \right\rangle \kappa_o^{p-3} \frac{(p-3)\,\Gamma\left(\frac{p}{2}\right)}{(2\pi)^{3/2}\Gamma\left(\frac{p-1}{2}\right)} \exp\left(-\frac{\kappa^2}{\kappa_i^2}\right)\left(\kappa_o^2 + \kappa^2\right)^{-p/2}. \tag{6}$$

3. The Variance of Amplitude Fluctuations With Aperture Averaging

3.1 Wave Equation for Random Media Propagation

As we have mentioned in Section 2.1, the dielectric constant of the coronal turbulence fluctuated due to the fluctuations of the solar wind. According to the wave propagation theory, the solar wind plasma irregularities will result in scattering and refraction of the link signals, leading to fluctuations in both amplitude and phase. These are adverse effects to the communication link and they can even cause the loss of the signal at the receiver. Note that only amplitude fluctuations is considered here and the phase fluctuations are beyond the scope of this paper.

When the optical waves encounter a turbulent solar wind eddy, the signal will be diffracted. In this paper, we consider a weak-to-moderate scattering situation and the refractive scintillation is

ignored. According to the former research, the amplitude fluctuation can be explicitly written as

$$\chi = -k^2 \int d^3 r \delta\varepsilon (r, t) A (R, r). \tag{7}$$

where $k = 2\pi/\lambda$ is the wavenumber and λ denotes the wavelength of the signal. $\delta\varepsilon = \frac{1}{\pi} r_e \lambda^2 \delta N_e$ represents the fluctuation of relative dielectric constant [3], r_e is the classical electron radius. In addition, $A (R, r) = \Re[G (R, r) \frac{E_0(r)}{E_0(R)}]$ reflects the real part of the Green function $G (R, r)$ and the ratio of electric field $\frac{E_0(r)}{E_0(R)}$.

3.2 Amplitude Fluctuations Variance With Aperture Averaging

The amplitude fluctuations are normally described using the log-amplitude and the log-amplitude variance. Because the average value of log-amplitude is zero, we use the log-amplitude variance as the first measure of an essential parameter to describing the variability of the optical waves. In this section, the covariance of amplitude fluctuations for optical waves propagating through coronal plasma is used to study the variance of amplitude fluctuations. The expressions of the variance of amplitude fluctuations have been derived by Ma *et al.* and Xu *et al.* [11], [19] with different forms for the case of optical waves in atmospheric turbulence and coronal turbulence, respectively. To analyze the effect of antenna aperture averaging on the amplitude fluctuations, in this paper we continue to use our previous proposed fluctuation expression and derive the final amplitude fluctuations of the signal received by the antenna. The detailed derivation is provided in the Appendix and the variance of the amplitude fluctuations is given by

$$\left\langle \chi^2 \right\rangle = 16\pi^4 r_e^2 k^{-2} \int_0^\infty \kappa d\kappa \int_0^L dz \sin^2 \left(\frac{z\kappa^2}{2k} \right) \Phi_N (\kappa, z) \left[\frac{2J_1 (\kappa a_r)}{\kappa a_r} \right]^2, \tag{8}$$

where a_r is the antenna radius, $J_1 (\cdot)$ denotes the first order Bessel function. For the sake of simplicity, the symbol for ensemble average of realization, $\langle \cdot \rangle$, is omitted in the following calculation.

Note that the last quadratic term in (8) is the wavenumber weighting function. Due to the aperture averaging effect, the influence of coronal turbulence on the variance of the amplitude fluctuations will be suppressed when the turbulent eddy size is smaller than antenna aperture. According to [26], this can be further approximated by the simplified Gaussian pattern:

$$\left[\frac{2J_1 (\kappa a_r)}{\kappa a_r} \right]^2 \approx \exp \left(-b^2 \kappa^2 a_r^2 \right), \tag{9}$$

where b is the coefficient and can be achieved through curve fitting with $b = 0.4832$ for Kolmogorov turbulence case or theoretically calculation with $b = 0.5216$. According to (9), the aperture averaging effect is only related to the receiver antenna itself. In addition, we have extended our research to the actual circumstance for optical waves transmit through non-Kolmogorov turbulence. Therefore, we choose $b = 0.5216$ in this paper [27].

By considering the triangular transformation, $\sin^2(\frac{z\kappa^2}{2k}) = \frac{1}{2}[1 - \cos(\frac{z\kappa^2}{k})]$, and substituting the coronal turbulence spectrum in (6) into (8), the variance of amplitude fluctuations for optical waves propagating through coronal turbulence can be rewritten as

$$\begin{aligned} \left\langle \chi^2 \right\rangle = {} & 8\pi^4 r_e^2 k^{-2} \frac{(p - 3)\, \Gamma \left(\frac{p}{2} \right)}{(2\pi)^{3/2} \Gamma \left(\frac{p - 1}{2} \right)} \kappa_0^{p-3} \\ & \cdot \left\{ \begin{array}{l} \int_0^L dz \int_0^\infty \kappa d\kappa \eta^2 N_e^2 (r) \exp \left(-\frac{\kappa^2}{\kappa_l^2} - b^2 \kappa^2 a_r^2 \right) \left(\kappa_0^2 + \kappa^2 \right)^{-p/2} \\ - \int_0^L \cos \left(\frac{z\kappa^2}{k} \right) dz \int_0^\infty \kappa d\kappa \eta^2 N_e^2 (r) \exp \left(-\frac{\kappa^2}{\kappa_l^2} - b^2 \kappa^2 a_r^2 \right) \left(\kappa_0^2 + \kappa^2 \right)^{-p/2} \end{array} \right\}. \end{aligned} \tag{10}$$

For convenience of formula derivation, the integral items are divided as the minus of I_1 and I_2.

$$I_1 = \int_0^L dz \int_0^\infty \kappa d\kappa \eta^2 N_e^2(r) \exp\left(-\frac{\kappa^2}{\kappa_i^2} - b^2\kappa^2 a_r^2\right)\left(\kappa_o^2 + \kappa^2\right)^{-p/2}, \tag{11}$$

$$I_2 = \int_0^L \cos\left(\frac{z\kappa^2}{k}\right) dz \int_0^\infty \kappa d\kappa \eta^2 N_e^2(r) \exp\left(-\frac{\kappa^2}{\kappa_i^2} - b^2\kappa^2 a_r^2\right)\left(\kappa_o^2 + \kappa^2\right)^{-p/2}, \tag{12}$$

We further use the following confluent hypergeometric function of the second kind [28]

$$U(a;c;x) = \frac{1}{\Gamma(a)} \int_0^\infty t^{a-1} \exp(-xt)(1+t)^{c-a-1} dt, \tag{13}$$

and then let $a = 1$, $x = \kappa_o^2\left(1/\kappa_i^2 + b^2 a_r^2\right)$, $c = 2 - p/2$, the I_1 term can then be simplified as

$$I_1 = \frac{\eta^2 N_e^2(r)}{2} \kappa_o^{2-p} \int_0^L dz U\left(1; 2 - \frac{p}{2}; \frac{\kappa_o^2}{\kappa_i^2} + \kappa_o^2 b^2 a_r^2\right). \tag{14}$$

Using Euler's formula, $\cos(x) = \Re[\exp(-ix)]$, and letting $a = 1$, $x = \kappa_o^2/\kappa_i^2 + b^2 a_r^2 \kappa_o^2 + i\kappa_o^2 z/k$, $c = 2 - p/2$, then I_2 term can be recast as

$$I_2 = \frac{\eta^2 N_e^2(r)}{2} \kappa_o^{2-p} \Re\left[\int_0^L dz \cdot U\left(1; 2 - \frac{p}{2}; \frac{\kappa_o^2}{\kappa_i^2} + b^2 a_r^2 \kappa_o^2 + i\frac{\kappa_o^2 z}{k}\right)\right] \quad . \tag{15}$$

where $\Re$ is the real part function.

Given that the inner scale of the solar wind turbulence is far less than its outer scale, $l_i \ll L_o$, and $\left|\kappa_o^2/\kappa_i^2\right| \ll 1$, then the confluent hypergeometric function can be further simplified as [29]

$$U(a;c;x) = \frac{\Gamma(c-1)}{\Gamma(a)} x^{1-c}, |x| \ll 1, \tag{16}$$

By inserting (16) into (14) and (15), respectively, and then taking these results into (10), a simplified amplitude fluctuations variance can be obtained as

$$\begin{aligned}\left\langle \chi^2 \right\rangle = {} & 4\pi^4 r_e{}^2 k^{-2} \frac{(p-3)\Gamma\left(\frac{p}{2}\right)\Gamma\left(1-\frac{p}{2}\right)}{(2\pi)^{3/2}\Gamma\left(\frac{p-1}{2}\right)} \kappa_o^{-1} \eta^2 N_e^2(r) \\ & \cdot \Re\left[\int_0^L \left(\frac{\kappa_o^2}{\kappa_i^2} + \kappa_o^2 b^2 a_r^2\right)^{p/2-1} dz - \int_0^L \left(\frac{\kappa_o^2}{\kappa_i^2} + b^2 a_r^2 \kappa_o^2 + i\frac{\kappa_o^2 z}{k}\right)^{p/2-1} dz\right].\end{aligned} \tag{17}$$

Note that, the first integration can be directly reduced to

$$Z_1 = \int_0^L \left(\frac{\kappa_o^2}{\kappa_i^2} + \kappa_o^2 b^2 a_r^2\right)^{p/2-1} dz = L\left(\frac{\kappa_o^2}{\kappa_i^2} + \kappa_o^2 b^2 a_r^2\right)^{p/2-1} \quad , \tag{18}$$

By evaluating the second integration in (17) with the following generalized hypergeometric function [28] as shown in (19) and letting $a = 1 - p/2$, $b = 1$, $c = 2$, $z = -i\kappa_i^2 L/(k + k\kappa_i^2 b^2 a_r^2)$, then it can be recast as

$${}_2F_1(a;b;c;z) = \frac{\Gamma(c)}{\Gamma(b)\Gamma(c-b)} \int_0^1 t^{b-1}(1-t)^{c-b-1}(1-zt)^{-a} dt, c > b > 0, \tag{19}$$

$$Z_2 = \frac{L}{\Gamma(2)}\left(\frac{\kappa_o^2}{\kappa_i^2} + b^2 a_r^2 \kappa_o^2\right)^{p/2-1} {}_2F_1\left(1 - \frac{p}{2}; 1; 2; -\frac{i\kappa_i^2 L}{k + kb^2 a_r^2 \kappa_i^2}\right), \tag{20}$$

Consequently, the final expression for optical waves propagating through non-Kolmogorov coronal turbulence is obtained by substituting (18) and (20) into (17).

$$\langle \chi^2 \rangle = 4\pi^4 r_e{}^2 k^{-2} \frac{(p-3)\,\Gamma\left(\frac{p}{2}\right)\Gamma\left(1-\frac{p}{2}\right)}{(2\pi)^{3/2}\Gamma\left(\frac{p-1}{2}\right)} \eta^2 N_e^2(r)\, L \left(1+\kappa_i^2 b^2 a_r^2\right)^{p/2-1} \frac{\kappa_o^{p-3}}{\kappa_i^{p-2}}$$
$$\cdot\, \Re\left[1 - \frac{1}{\Gamma(2)}{}_2F_1\left(1-\frac{p}{2};1;2;\frac{-i\kappa_i^2 L}{k\left(1+\kappa_i^2 b^2 a_r^2\right)}\right)\right]. \tag{21}$$

It should be emphasized that the derived closed-form amplitude fluctuations model takes account of the finite aperture receiver. By means of this formula, the influence of turbulence outer scale, L_o, inner scale, l_i, spectral index, p, and the antenna radius, a_r, on the fluctuations can be analyzed quantitatively. In addition, the scintillation index, m, which characterize the signal intensity deviation normalized to the average intensity, can be also achieved and is a critical parameter for the following BER performance prediction. After all, the main contribution of this subsection can be concluded that a tractable and closed-form expression for the variance of amplitude fluctuations is proposed in this paper, which has not been studied to the best of our knowledge. In addition, the proposed expressions reveal that the variation of turbulent outer scale, inner scale, spectral index, and antenna radius have an obvious impact on the amplitude fluctuations.

4. BER Performance in GG Coronal Turbulence Channel

To evaluate the effect of coronal parameters on the FSO system, we only consider the IM/DD links with the on-off keying (OOK) scheme in this paper. The noise is modeled as the additive white Gaussian noise (AWGN), its mean value and variance are zero and $N_0/2$, respectively. As we have mentioned in Section 1, the GG channel model can well characterize the coronal channel, both in weak scintillation and in moderate scintillation. Therefore, the GG distribution is adopted in this paper because we mainly consider the weak-to-moderate scintillation. Following [17], the so-called GG channel model can be written as

$$f_I(I) = \frac{2(\phi\varphi)^{(\phi+\varphi)/2}}{\Gamma(\phi)\,\Gamma(\varphi)} I^{(\phi+\varphi)/2-1} K_{\phi-\varphi}\left(2\sqrt{\phi\varphi I}\right), I > 0, \tag{22}$$

with $K_x(\cdot)$ as the x-th order modified Bessel function of the second kind and $\Gamma(\cdot)$ is the standard gamma function. Note that ϕ and φ are the effective number of small scale and large scale eddies of the coronal scattering environment, respectively. These parameters can be specified as functions of the variance of amplitude fluctuations, χ^2, according to the solar corona turbulence conditions [18]

$$\phi = \left\{\exp\left[\frac{0.49\chi^2}{\left(1+0.18d^2+0.56\chi^{12/5}\right)^{7/6}}\right]-1\right\}^{-1}, \tag{23}$$

$$\varphi = \left\{\exp\left[\frac{0.51\chi^2\left(1+0.69\chi^{12/5}\right)^{-5/6}}{1+0.9d^2+0.62d^2\chi^{12/5}}\right]-1\right\}^{-1}. \tag{24}$$

where $d = \sqrt{\pi D^2/(2\lambda L)}$, D denotes the diameter of the receiver aperture. Therefore, the scintillation index for the GG channel model, which is defined as the intensity standard deviation normalized to the average received intensity, can be further written as

$$m = \frac{E\left[I^2\right] - (E[I])^2}{(E[I])^2} = \frac{1}{\phi} + \frac{1}{\varphi} + \frac{1}{\phi\varphi}. \tag{25}$$

The related BER of the optical waves transmitted in a GG distributed channel is for optimized detection and is given by [20]

$$BER = \int_0^\infty f_I(I) \cdot \frac{1}{2} erfc\left(\frac{\mu I}{2\sqrt{N_0}}\right) dI, \tag{26}$$

Note that $K_v(\cdot)$ in (22) and the complementary error function $erfc(\cdot)$ in (26) can be recast by the Meijer-G function [30]

$$K_v(x) = \frac{1}{2} G_{0,2}^{2,0}\left[\frac{x^2}{4}\middle|\begin{matrix}-\\ \frac{v}{2}, -\frac{v}{2}\end{matrix}\right], \; erfc\left(\sqrt{x}\right) = \frac{1}{\sqrt{\pi}} G_{1,2}^{2,0}\left[x\middle|\begin{matrix}1\\ 0, \frac{1}{2}\end{matrix}\right]. \tag{27}$$

Here, $G_{p,q}^{m,n}[\cdot]$ is the Meijer-G function. By substituting (22) and (27) into (26), the average BER can be finally written as

$$BER = \frac{2^{\phi+\varphi-3}}{\pi^{3/2}\Gamma(\phi)\Gamma(\varphi)} G_{5,2}^{2,4}\left[\frac{4\mu}{\phi^2\varphi^2}\middle|\begin{matrix}\frac{1-\phi}{2}, \frac{2-\phi}{2}, \frac{1-\varphi}{2}, \frac{2-\varphi}{2}, 1\\ 0, \frac{1}{2}\end{matrix}\right]. \tag{28}$$

where $\mu = \tau^2/N_0$. Here, τ is the photoelectric conversion efficiency.

In conclusion, a closed-form BER formula is derived to facilitate the calculation. The proposed BER model considers the link performance of optical waves propagation through coronal turbulence, which is a serious problem with the development of deep space exploration. In addition, we investigated the link BER with the assumption of weak-to-moderate scintillation under GG channel distribution model.

5. Numerical Evaluations and Discussion

Numerical evaluations are conducted in this section to investigate the effect of coronal parameters on amplitude fluctuations of optical waves propagation through coronal turbulence and the BER performance over coronal turbulence channel. We mainly consider Earth to Mars communication in this paper. Therefore, we set $L_{sp} = 1.5L_{se}$ as appropriate for Mars' orbit during superior solar conjunction. Note that $L_{se} = 1.5 \times 10^8$ km. For simplicity, the SPE angle and relative solar wind density fluctuation factor are fixed as $\beta = 0.3^\circ$ and $\eta = 5\%$, respectively. According to the former Mars exploration missions [1], the wavelength is set as $\lambda = 532$ nm, 880 nm, 1064 nm, and 1550 nm. In addition, the antenna radius is choosing as $a_r = 0.2$ m, 1.2 m and 5 m, respectively. Unless otherwise specified, the other parameters used in the calculations are assumed as following: SEP angle $0.35^\circ < \alpha < 0.55^\circ$; spectral index $3 < p < 4$; outer scale 1×10^5 km $< L_o < 1 \times 10^7$ km; inner scale 2×10^3 km $< l_i < 6 \times 10^3$ km.

The impact of aperture averaging and SEP angle on the scintillation index and the BER of optical waves propagation in coronal turbulence are demonstrated in Fig. 2. The horizontal axes in Fig. 2(b) and (c) denote the average signal-to-noise ratio (SNR_0). As we can see in Fig. 2(a), the scintillation index increases slowly with the initial decrease in SEP angle, and it increases steeply when α is sufficiently small. In addition, the scintillation intensity enters into moderate turbulence region when $\alpha = 0.4^\circ$ and even into strong turbulence region when α continues to decrease. Moreover, the scintillation index decreases with the increase of antenna radius. This phenomenon is more obvious when α trends to its minimum. This can be explained from the following physical point of views: First, both the solar wind density and its fluctuation intensity increase with the decease of heliocentric distance, r. This phenomenon is reinforced because the density and its fluctuation intensity have exponential relationship with r according to (4) and (5). Therefore, the optical signal will encounter more turbulence irregularities, and sustain more scintillation effect. Second, the aperture averaging effect is enhanced along with the increase of a_r. This behavior is similar to the classical amplitude fluctuations of optical waves propagation in atmosphere turbulence with different antenna radii.

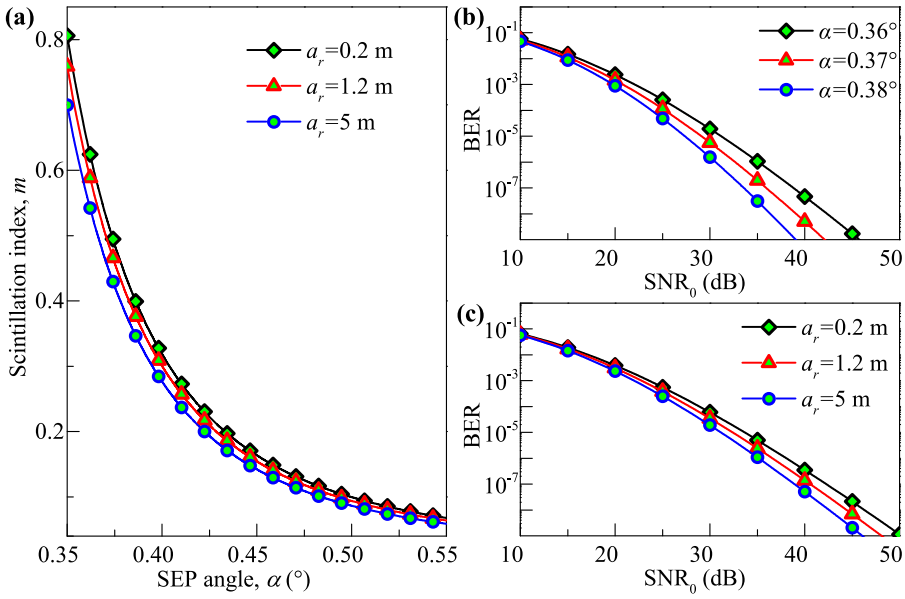

Fig. 2. (a) The scintillation index versus a_r for different SEP angles (b) the BER performance against SEP angle (c) the BER performance against a_r.

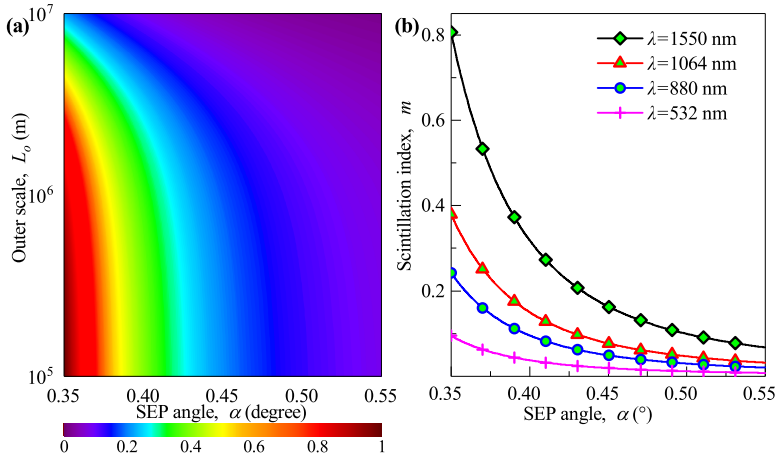

Fig. 3. (a) Normalized amplitude fluctuations dependence on both outer scale and SEP angle (b) the scintillation index against optical wavelength under different SEP angles.

According to the above description, the BER also decreases with the increase of SEP angle and antenna radius as shown in Fig. 2(b) and (c). This tendency is more obvious when SNR_0 increases.

Fig. 3 exhibits the effect of outer scale on the normalized amplitude fluctuations and the impacts of optical wavelength on the scintillation index. The color bar at the bottom of Fig. 3(a) denotes the normalized amplitude fluctuations value. It is shown that the normalized amplitude fluctuations decrease with the increase of outer scale. This phenomenon can be interpreted due to the focusing effect of the outer scale. This is more prominent with the increase of SEP angle because the size of outer scale increases with the increase of heliocentric distance or SEP angle. As shown in Fig. 3(b), the scintillation index with larger λ is more affected by coronal turbulence than those with smaller λ. This conclusion is reasonable because the spatial coherence length is proportional to the wavelength. Therefore, the scintillation effect caused by coronal turbulence can be more

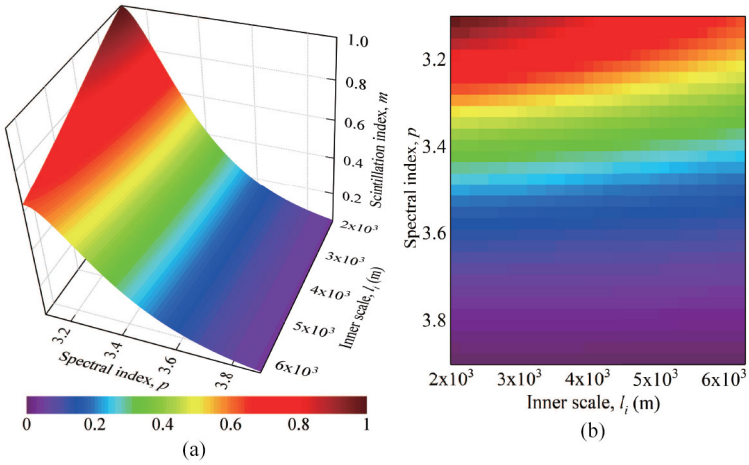

Fig. 4. (a) Normalized amplitude fluctuations dependence on both inner scale and spectral index (b) the corresponding planform.

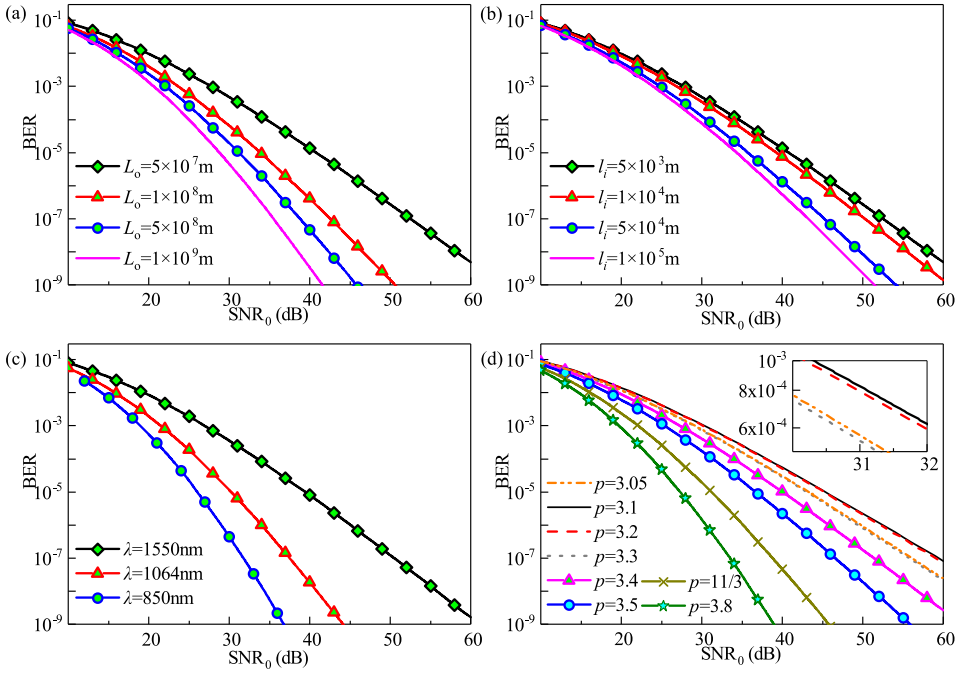

Fig. 5. The BER performance verse different parameters (a) outer scale, (b) inner scale, (c) wavelength, and (d) spectral index.

effectively mitigated with small optical wavelength. This conclusion further confirms thatdecreasing the wavelength can potentially improve the link performance for future deep space FSO communication.

Because the lower limit of the turbulence inertial range is determined by the inner scale, the strength of coronal turbulence will be enhanced with the decrease of outer scale. In this case, the optical waves encounter more turbulence eddies along their communication link. Consequently, the normalized amplitude fluctuations increase monotonically with the decrease of inner scale, as depicted in Fig. 4. To analyze the effect of non-Kolmogorov spectrum with different spectral indexes, the amplitude fluctuations verse spectral index is also demonstrated in Fig. 4. The simulation results reveal that the spectral index has a significant impact on the amplitude fluctuations. The amplitude

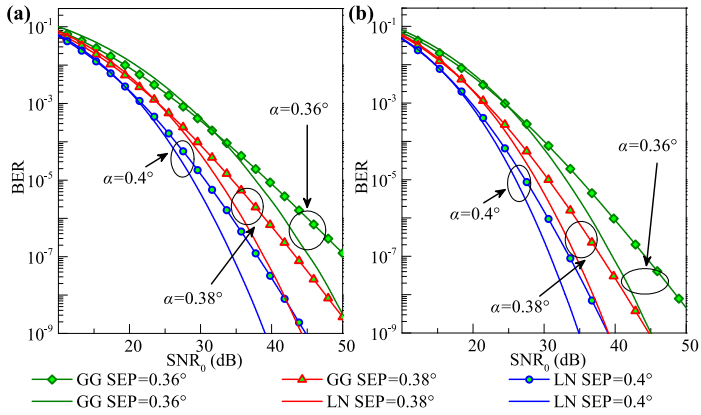

Fig. 6. The BER performance of the link with GG channel model and LN channel model under different SEP angles at (a) $\lambda = 1550$ nm and (b) $\lambda = 1064$ nm.

fluctuations usually decrease with the increase of spectral index. It should be emphasized that the normalized amplitude fluctuations first increase to its maximum from 3.05 to 3.1 and then decrease sharply when the spectral index increase from 3.1 to 3.3. However, this tendency slows down as the spectral index increases from 3.3 to 3.9 and the amplitude fluctuations finally go to zero during this period. These results are similar with the optical waves propagation in atmospheric turbulence and the radio waves passing through the ionospheric irregularities.

Fig. 5 explores the BER performance of the FSO communication system for optical waves propagation through coronal turbulence under various parameters. Both the outer scale and the inner scale induce rather profound influence on the BER performance, as shown in Fig. 5(a) and (b), respectively. The BER decreases with the increase of outer scale and inner scale apparently. For instance, the receiver, which is working at $\mathrm{SNR}_0 = 30$ dB, needs another 6 dB to achieve the same BER performance when the outer scale decreases from 1×10^9 m to 1×10^8 m. This tendency is more obvious with the increase of SNR_0 and it can be also achieved for different inner scale. Compared 5(a) with (b), we can find that the inner scale have a more significant impact on the BER performance to some extent. Therefore, we conclude that the inner scale should be also taken account in the future deep space FSO communication due to the effect of solar scintillation.

As expected, the BER can be effectively reduced by decreasing the optical wavelength, as shown in Fig. 5(c). This result is similar to our former research in [11]. Therefore, decreasing the wavelength or increasing the carrier frequency are alternative methods to eliminate the coronal turbulence effect on the communication performance. In addition, the spectral index induces a complicated effect on the BER performance, as shown in Fig. 5(d). The BER falls down quickly when p increases from 3.3 to 3.8. However, it increases to its maximum first when p increases from 3.05 to 3.1, and then decreases from 3.1 to 3.3. This phenomenon is amplified in the inner figure of Fig. 5(d).

To evaluate the deep space FSO communication link performance with our proposed amplitude fluctuations model, which considers the aperture averaging effect, the BER performance under GG and LN channel models are depicted in Fig. 6. It is clear that BER decreases with the increase of SEP angle both in Fig. 6(a) and (b) with $\lambda = 1550$ nm and $\lambda = 1064$ nm, respectively. Comparing Fig. 6(a) with (b), the BER performance is apparently enhanced under the same SNR_0 value. These results can be also achieved in Fig. 2(b) and Fig. 3(b), and have been explained previously.

Even though the curves with these models have the same tendency, they exhibit rather different value with the variation of SEP angle. For instance, in order to achieve the same BER performance at $\mathrm{BER}_0 = 10^{-9}$, the SNR_0 only need 39 dB with the LN model when $\alpha = 0.4^\circ$ and $\lambda = 1550$ nm, while the penalty rises to 42.8 dB when we consider with GG model. However, a normalized SNR_0 of approximately 9.5 dB is needed to obtain the same BER when $\alpha = 0.38^\circ$ and $\lambda = 1550$ nm. This tendency is further strengthened when α decreases to 0.36°. It can be finally concluded that the BER performance under our proposed model with GG model is closer to the actual situation.

We generally believe that this is reasonable since solar scintillation enters into a moderate region and even strong region when α decreases from 0.4° according to Fig. 2(a). Therefore, both our proposed amplitude fluctuations model and BER performance model under GG channel model can be applied in the future deep space FSO communication during superior solar conjunction.

In light of these simulations, our proposed amplitude fluctuations model can be used to predict the amplitude fluctuations caused by coronal turbulence irregularities. Meanwhile, the FSO link performance under GG channel model is forecast by our proposed BER prediction formula. Some schemes can be applied to decrease the impact of solar scintillation on the link performance, such as enhancing the antenna radius and decreasing the optical wavelength. However, these schemes have run into a bottleneck due to the engineering constraint. Therefore, there is a great need for an efficient scheme for the future deep space FSO communication.

Given that the amplitude fluctuations are caused by solar wind irregularities, a precise density model and fluctuation model are crucial to the amplitude fluctuations. Unfortunately, all of these models are mainly based on observations and assumptions but not a solid foundation of theory. In addition, the Taylor's frozen theory used in this paper may not be perfectly valid in all the coronal space since the exact coronal environment is still a mystery. Under such circumstances, our research is still in infancy and the proposed amplitude fluctuations model with the wildly used solar wind density model need further study.

6. Conclusion

This paper proposed an amplitude fluctuations model to investigate the impact of coronal turbulence on optical waves propagation for deep space communication. Considering weak-to-moderate coronal turbulence channels, the GG distribution model is further used to evaluate the average BER of FSO link. The influence of aperture averaging on the performance of FSO communication system is further studied. The effect of coronal parameters, namely spectral index, turbulent outer scale and inner scale, on the amplitude fluctuations and BER performance are also quantitatively investigated. It is found that an increase in antenna radius decreases the amplitude fluctuations first and this results in BER performance improvement. As the spectral index increases, both amplitude fluctuations and BER increase to their maximum sharply, and then gradually decrease. Moreover, the performance of FSO link degraded more severely with the decrease of turbulence inner scale and outer scale. Decreasing the optical wavelength and enlarging the antenna radius are optional ways to mitigate the influence of coronal turbulence and finally improve the FSO communication performance to some extent due to the technological restriction. Therefore, this study provides a theoretical foundation and design basis for the FSO communication system in future deep space exploration.

Appendix

According to our previous derivation of amplitude fluctuations for the optical waves in coronal turbulence [11], the amplitude fluctuations measured at different space in the antenna can be written as

$$\langle \chi(R)\,\chi(R+\Delta\rho)\rangle = r_e^2\lambda^4k^2\int_0^L dz\sin^2\left(\frac{z\kappa^2}{2k}\right)\int_0^\infty \kappa d\kappa\Phi_N(\kappa)\,J_0(\kappa\Delta\rho)\,. \tag{29}$$

where $J_0(\kappa\Delta\rho)$ is the combination of the surface element. Just as shown in Fig. 7, $\Delta\rho=\rho_1-\rho_2$ denotes the displacement vector. Considering a receiver with antenna radius, a_r, the variance of amplitude fluctuations is an integration over the aperture as

$$\langle\chi^2\rangle=\frac{r_e^2\lambda^4k^2}{A^2}\int_A\int d^2\sigma_1\int_A\int d^2\sigma_2\int_0^L dz\sin^2\left(\frac{z\kappa^2}{2k}\right)\int_0^\infty \kappa d\kappa\Phi_N(\kappa)\,J_0(\kappa\,|\sigma_1-\sigma_2|)\,, \tag{30}$$

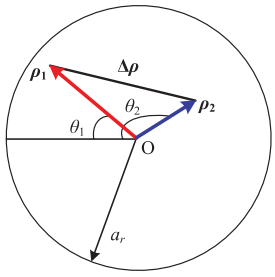

Fig. 7. The 2-D antenna aperture with two surface elements.

where $A = \pi {a_r}^2$ denotes to the antenna area. The integration result in the entire antenna surface is further recast as

$$\langle \chi^2 \rangle = \frac{{r_e}^2 \lambda^4 k^2}{\pi^2 {a_r}^4} \int_0^{a_r} \rho_1 d\rho_1 \int_0^{2\pi} d\theta_1 \int_0^{a_r} \rho_2 d\rho_2 \int_0^{2\pi} d\theta_2 J_0 \left(\kappa \sqrt{{\rho_1}^2 + {\rho_2}^2 - 2\rho_1 \rho_2 \cos(\theta_2 - \theta_1)} \right) \cdot \int_0^{\infty} \kappa d\kappa \Phi_N(\kappa) \int_0^{L} dz \sin^2 \left(\frac{z\kappa^2}{2k} \right), \tag{31}$$

According to the following Bessel function [29]

$$J_0 \left(\kappa \sqrt{{\rho_1}^2 + {\rho_2}^2 - 2\rho_1 \rho_2 \cos(\theta_2 - \theta_1)} \right) = \sum_0^{\infty} \varepsilon_n J_n(\kappa \rho_1) J_n(\kappa \rho_2) \cos[n(\theta_2 - \theta_1)], \tag{32}$$

we have

$$J_0 \left(\kappa \sqrt{{\rho_1}^2 + {\rho_2}^2 - 2\rho_1 \rho_2 \cos(\phi_2 - \phi_1)} \right) = J_0(\kappa \rho_1) J_0(\kappa \rho_2), \tag{33}$$

Note that, $\varepsilon_n = 1$ is applied in (32), when $n = 0$. By substituting (33) into (31), the amplitude fluctuations can be written as

$$\langle \chi^2 \rangle = \frac{4{r_e}^2 \lambda^4 k^2}{{a_r}^2} \int_0^{a_r} \frac{J_0(\kappa \rho_1) \rho_1 d\rho_1}{a_r} \int_0^{a_r} \frac{J_0(\kappa \rho_2) \rho_2 d\rho_2}{a_r} \int_0^{\infty} \kappa d\kappa \Phi_N(\kappa) \int_0^{L} dz \sin^2 \left(\frac{z\kappa^2}{2k} \right), \tag{34}$$

Since $\int_0^a x J_0(x\kappa)\, dx / a^2 = J_1(\kappa a)/\kappa a$, therefore, the variance of amplitude fluctuations for optical waves passing through coronal turbulence with aperture averaging effect can be finally expressed as

$$\langle \chi^2 \rangle = 16\pi^4 {r_e}^2 k^{-2} \int_0^{\infty} \kappa d\kappa \int_0^{L} dz \sin^2 \left(\frac{z\kappa^2}{2k} \right) \Phi_N(\kappa, z) \left[\frac{2J_1(\kappa a_r)}{\kappa a_r} \right]^2. \tag{35}$$

Note that, $[2J_1(\kappa a_r)/\kappa a_r]^2$ is the weighting function due to aperture averaging effect, it acts like a low-pass filter and is also referred to Airy function.

References

[1] H. Kaushal and G. Kaddoum, "Optical communication in space: Challenges and mitigation techniques," *IEEE Commun. Surv. Tut.*, vol. 19, no. 1, pp. 57–96, Aug. 2017.
[2] Y. Sun, C. Gong, Z. Xu, and Y. Zhan, "Link gain and pulse width broadening evaluation of non-line-of-sight optical wireless scattering communication over broad spectra," *IEEE Photon. J.*, vol. 9, no. 3, Jun. 2017, Art. no. 7900212.
[3] G. Xu and Z. Song, "A new model of amplitude fluctuations for radio propagation in solar corona during superior solar conjunction," *Radio Sci.*, vol. 51, no. 2, pp. 71–81, Dec. 2016.
[4] Y. Feria, M. Belongie, T. McPheeters, and H. Tan, "Solar scintillation effects on telecommunication links at Ka-band and X-band," TDA Progress Report 42–129, May 1997. [Online]. Available: https://www.ipnpr.jpl.nasa.gov/progress_report/42-129/129.pdf

[5] D. D. Morabito, "Solar corona-induced fluctuations on spacecraft signal amplitude observed during solar superior conjunctions of the Cassini spacecraft," *Radio Sci.*, vol. 42, no. 3, Jun. 2007, Art. no. RS3002.
[6] Q. Li, L. Yin, and J. Lu, "Performance study of a deep space communications system with low-density parity-check coding under solar scintillation," *Int. J. Commun.*, vol. 6, no. 1, pp. 1–9, Apr. 2012.
[7] D. D. Morabito, S. Shambayati, S. Finley, and D. Fort, "The cassini may 2000 solar conjunction," *IEEE Trans. Antennas Propag.*, vol. 51, no. 2, pp. 201–219, Apr. 2003.
[8] C. M. Ho and A. Wheelon, "Amplitude scintillation due to atmospheric turbulence for the Deep Space Network Ka-band downlink," California Inst. Technol., Pasadena, CA, USA, Interplanetary Network Progress Report 42-158, Aug. 2004. [Online] Available: http://adsabs.harvard.edu/abs/2004IPNPR.158E...1H
[9] G. M. Calves, S. V. Pogrebenko, G. Cimo, and D. A. Duev, "Observations and analysis of phase scintillation of spacecraft signal on the interplanetary plasma," *Astron. Astrophys.*, vol. 564, no. A4, pp. 275–291, Mar. 2014.
[10] A. I. Efimov, N. A. Armand, L. A. Lukanina, L. N. Samoznaev, I. V. Chashei, and M. K. Bird, "Radial dependence of the level of amplitude fluctuations of spacecraft radio signals probing circumsolar plasma," *J. Commun. Technol. Electron.*, vol. 53, no. 10, pp. 1186–1194, Oct. 2008.
[11] G. Xu and Z. Song, "Solar scintillation effects on the deep space communication performance for radio wave propagation through non-Kolmogorov turbulence," *IEEE Antennas Wireless Propag. Lett.*, vol. 17, no. 8, pp. 1505–1509, Aug. 2018.
[12] G. Xu and Z. Song, "Phase fluctuations model for EM wave propagation through solar scintillation at superior solar conjunction," *Waves Random Complex Media*, vol. 27, no. 2, pp. 272–288, Feb. 2017.
[13] A. I. Efimov, I. V. Chashei, M. K. Bird, L. N. Samoznaev, and D. Plettemeier, "Turbulence in the inner solar wind determined from frequency fluctuations of the downlink signals from the ulysses and galileo spacecraft," *Astron. Rep.*, vol. 49, no. 6, pp. 485–494, Jun. 2005.
[14] P. Manoharan, "Ooty interplanetary scintillation-remote-sensing observations and analysis of coronal mass ejections in the heliosphere," *Sol. Phys.*, vol. 265, no. 1/2, pp. 137–157, Aug. 2010.
[15] G. Xu and Z. Song, "Effects of solar scintillation on deep space communications: challenges and prediction techniques," *IEEE Wireless Commun.*, vol. 26, no. 2, pp. 10–16, Apr. 2019.
[16] G. Xu, "Error performance of deep space optical communication with M-ary pulse position modulation over coronal turbulence channels," *Opt. Exp.*, vol. 27, no. 9, pp. 13344–13356, Apr. 2019.
[17] B. Epple, "Simplified channel model for simulation of free-space optical communications," *J. Opt. Commun. Netw.*, vol. 2, no. 5, pp. 293–304, May 2010.
[18] M. Uysal, L. Jing, and Y. Meng, "Error rate performance analysis of coded free-space optical links over gamma-gamma atmospheric turbulence channels," *IEEE Trans. Wireless Commun.*, vol. 5, no. 6, pp. 1229–1233, Jun. 2006.
[19] J. Ma, K. Li, L. Tan, S. Yu, and Y. Cao, "Performance analysis of satellite-to-ground downlink coherent optical communications with spatial diversity over Gamma-Gamma atmospheric turbulence," *Appl. Opt.*, vol. 54, no. 25, pp. 7575–7585, Sep. 2015.
[20] Y. Wang, F. Du, J. Ma, and L. Tan, "Employing circle polarization shift keying in free space optical communication with gamma-gamma atmospheric turbulence channel," *Opt. Commun.*, vol. 333, pp. 167–174, Dec. 2014.
[21] G. Thejappa and R. J. Macdowall, "Effects of scattering on radio emission from the quiet sun at low frequencies," *Astrophys. J.*, vol. 676, no. 2, pp. 1338–1345, Apr. 2008.
[22] C. M. Ho, D. D. Morabito, and R. Woo, "Solar corona effects on angle of arrival fluctuations for microwave telecommunication links during superior solar conjunction," *Radio Sci.*, vol. 43, no. 2, pp. 1–13, Apr. 2008.
[23] A. N. Afanasiev and N. T. Afanasiev, "Diagnostics of near-solar plasma turbulence parameters using the radio sounding technique at small heliocentric distances," *Sol. Phys.*, vol. 245, no. 2, pp. 355–367, Oct. 2007.
[24] A. D. Wheelon, *Electromagnetic scintillation. Part II. Weak scattering.* Cambridge, U.K.: Cambridge Univ. Press, 2003.
[25] Z. W. Xu, J. Wu, Z. S. Wu, and Q. Li, "Solution for the fourth moment equation of waves in random continuum under strong fluctuations: General theory and plane wave solution," *IEEE Trans. Antennas Propag.*, vol. 55, no. 6, pp. 1613-1621, Jun. 2007.
[26] L. Cui, X. Cao, B. Xue, and L. Cao, "Analysis of angle of arrival fluctuations for optical waves' propagation through weak anisotropic non-Kolmogorov turbulence," *Opt. Exp.*, vol. 23, no. 5, pp. 63136–6325, May 2015.
[27] Y. Cheon and A. Muschinski, "Closed-form approximations for the angle-of-arrival variance of plane and spherical waves propagating through homogeneous and isotropic turbulence," *J. Opt. Soc. America A-Opt. Image Sci. Vis.*, vol. 24, no. 2, pp. 415–422, Mar. 2007.
[28] M. Abramowitz and I. S. Stegun, *Handbook of Mathematical Functions with Formulas Graphs and Mathematical Tables*. Mineola, NY, USA: Dover, 2007.
[29] I. Gradshteyn and I. Ryzhik, *Table of Integrals, Series, and Products.* New York, NY, USA: Academic, 2007.
[30] W. Lim, C. Yun, and K. Kim, "BER performance analysis of radio over free-space optical systems considering laser phase noise under Gamma-Gamma turbulence channels," *Opt. Exp.*, vol. 17, no. 6, pp. 4479–4484, Mar. 2009.